

**投稿論文 (英文)**  
**PAPERS**

# DEFORMATIONAL RESISTANCE OF FRESH CONCRETE THROUGH BENT AND TAPERED PIPES

Anura S.M.NANAYAKKARA\*, Kazumasa OZAWA\*\*  
and Koichi MAEKAWA\*\*\*

This is to report on the resistance to deformation of fresh concrete when the rearrangement of constituent particles of fresh concrete, i.e., gravel, sand and cement, is introduced. For realizing the simple deformation field in shear, bent and tapered pipe units were adopted in test and stable flow of fresh concrete through them was produced. Herein, the pressure at the inlet of deformed pipes was measured as an indicator of deformability of fresh concrete, which is regarded as the particulate assembly with different sizes. The effect of volume fraction of gravel, sand and cementitious powder on the resistance to deformation was mainly focused in the series of test based upon the multi-phase concept of hydrodynamics. The sensitivity of volume fractions to the total deformational resistance of concrete was of experimental interest to the authors.

*Key Words* : fresh concrete, deformability, pumpability, multi-phase, mixture

## 1. INTRODUCTION

Recently rising are engineering demands for high-grade concrete at freshly mixed stage as well as the hardened<sup>1)</sup>. This is because the physical features of fresh concrete at the fluidized stage have closer linkage with rationalization of construction in practice. From time to time, construction systems have required some particular properties of fresh concrete to be fairly satisfied. Among expected performances, mechanical characteristics, especially associated with deformation of fresh concrete, are often rated at the top priority to be sought. Some versatile predictive method evaluating "deformability" of fresh concrete would be crucial so that we could realize the rational design of high performance concrete which requires high durability as well as the self-placable aspect in progress<sup>2)</sup>.

This paper is to study the deformability which indicates how much the external action be needed to induce specific rate of deformation. Hereafter, the deformation of fresh concrete is defined as the deformation involving rearrangement of solid particles suspended in concrete<sup>3)</sup>. Accordingly, the deformation follows the collision and friction among particles<sup>4)</sup>. This is the source of deformational resistance.

In the last decade, the authors have chiefly

\* Member of JSCE, Dr.Eng., Lecturer, Department of Civil Engineering, University of Moratuwa, Sri Lanka

\*\* Member of JSCE, Dr.Eng., Associate Professor, Department of Civil Engineering, The University of Tokyo (7-3-1, Hongo, Bunkyo-ku, Tokyo 113)

\*\*\* Member of JSCE, Dr.Eng., Associate Professor, Engineering Research Institute, The University of Tokyo (7-3-1, Hongo, Bunkyo-ku, Tokyo 113)

focused on quantifying of the field of deformation for multi-component material composed by suspended solid particles and liquid matrix<sup>5),6)</sup>. Through the spatial averaging procedure, the deformational field of dense solid-liquid was manifested in terms of strain tensors and their invariants based on Eulerian expression. As the second stage of development, this paper aims at constructing bridges between the rate of deformation and corresponding force which originates from the sum of interaction among particles.

The deformation of particulate solid-liquid as a fictitious model of fresh concrete was experimentally verified being in mode of pure shear and its intensity was found to be directly proportional to the rate of flow in tapered and bent pipes<sup>5),6)</sup>. In this paper, the authors report the pressure at the inlet of the deformed pipe units under the constant rate of flow. As mentioned above, the measured pressure results from the entire mechanical interaction among particles excited in shear mode whose magnitude is known<sup>5),6)</sup>. The authors adopted the pressure measured under specified intensity of shear rate realized in tapered and bent pipes as the index of deformability. Here, the pipe units were regarded as the device to reproduce the specified simple mode of deformation. The pressure needed under particular rate of flow represents some sort of "stiffness" for particle assembly with different dimensions<sup>7)</sup>.

In the series of test, the volume fractions of gravel, sand and cement powder were systematically assigned for investigating the sensitivity of each fraction of mixture to the deformational resistance. The authors in the past proposed the computational multi-phase model for fresh concrete<sup>8)</sup>. The

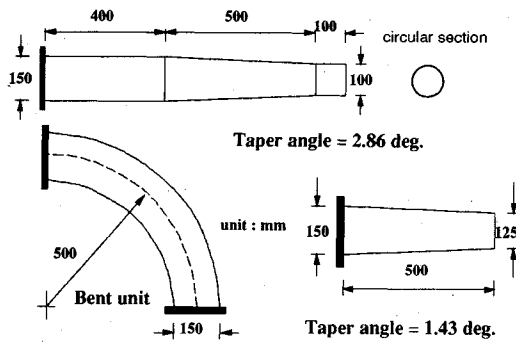


Fig.1 Dimensions of deformed pipe units.

experimental program was designed so that the particle interaction model could be performed on substantial development of modeling in future. This predictive method on deformability is expected to be one of theoretical backgrounds for mix design of high performance concrete.

## 2. EXPERIMENT

### (1) Deformability test of fresh concrete

Since the pure shear deformation of fresh concrete and its spatial extent are reproduced<sup>(5,6)</sup> at the bent and tapering particulate flow, the authors adopted the pump resistant test in using deformed units of bent and tapered pipes as shown in Fig.1. Under the enforced deformation, we can measure the pressure as an indicator of deformability.

First, the concrete was charged inside the bent and tapered units attached to the pump hydraulic cylinder and second, the input of new concrete was made with constant rate of flow through the straight pipe using laboratory scale pumping apparatus as shown in Fig.2<sup>9)</sup>. Under the stable flow and associated deformation of concrete, the pressure at the head of piston (See Fig.2) was indirectly measured by sensing the oil pressure inside the hydraulic cylinder as shown in Fig.2. As no inertia of internal rod to transfer pressure between oil and concrete can be assumed, we can apply the hydrostatic equilibrium for computing the total pressure to concrete from the oil hydraulic pressure.

The piston of the pump cylinder was inclined 20 degree from horizontal to prevent concrete from flowing out before starting experiments. Concrete was tamped gently when charged from the outlet into the pipe by using a rod with a circular disc. No vibration was introduced at the inside of the pump device.

The authors specified several levels of flow rate in order to impart data to the verification of the computational model in future, because the pressure needed to drive the motion of concrete is

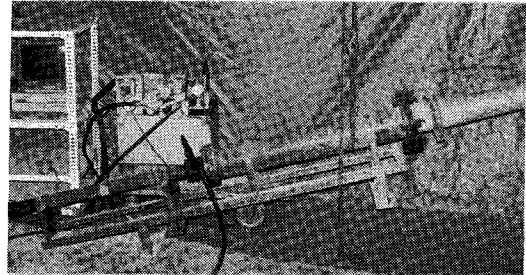
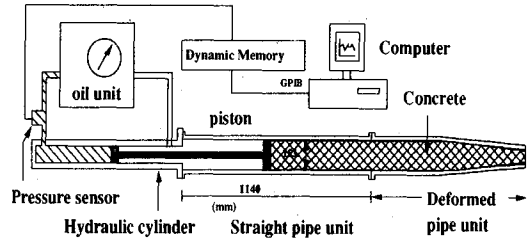


Fig.2 Pumping apparatus and measurement system.

not proportional to the rate of flow but nonlinear. During each test, however, the rate of flow was kept constant in time domain (about 5.0 cm/s) within  $\pm 0.1$  cm/s. Concerning the effect of mixture proportion on the pumpability, the authors selected test cases having the same rate of flow adopted.

For any concrete mixture, the authors measured the oil pressure by using dynamic data storage in time domain for two cases, 1) straight pipe only without any attached deformed pipe and 2) straight pipe + tapered or bent unit (deformed pipe), and obtained time averaged values ( $P_w$  and  $P_c$ ) as shown in Fig.3. The measurement took approximately 20 seconds. The pressure specified by  $P_c$  involves the effect of friction between the piston head and the wall of the straight pipe. Then, the value of  $(P_c - P_w)$  indicates the substantial pressure produced by the deformed pipe.

The total mean pressure applied to concrete is inversely proportional to the ratio of the sectional area of pistons in the straight pipe and the oil cylinder, that is equal to 1/0.215. Since our concern is the deformational resistance of concrete created at the bent or tapered units connected with the straight pipe, 0.215  $(P_c - P_w)$  as the total pressure was treated as the mechanical factor of the resistance to the deformation arising in the test domains in the deformed pipe units.

As shown in Fig.3, the fluctuation of measurement around the time averaged value was found. This may originate from the unstable touch of piston with the inner wall of the pipe and the local contact of particles which is not continuous but some sort of discrete events. As far as the multi-

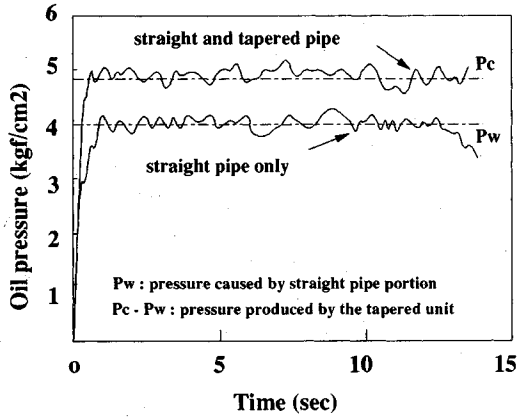


Fig.3 Time averaging of effective pressure.

phase theory and formulated compatibility of the particulate flow are concerned<sup>4)-6)</sup>, time averaged variables are explicitly defined and the variation in small time interval is implicitly taken into account with regard to the constitutive law for flow accompanying turbulence<sup>15)</sup>. Accordingly, we hereafter use the time averaged values of pressures.

(2) Parameters indicating mixtures of concrete

In this study, approximately 20 different mixtures of concrete were examined. River sand, river and crushed gravels were used as specified in Table 1. For powder materials, ordinary Portland cement, two types of blast furnace slag (Blaine value; 3000 and 8000 cm<sup>2</sup>/g) and fly ash were used. The super plasticizer was added approximately 1% of the powders by weight. The authors followed the conventional procedure of producing concrete. Here, the mixing time with the forced flat type mixer (100 liter) with a single rotor was specified 2 minutes after charging entire constituent materials. Because, plenty of mixture proportion can be ranked as high viscous concrete with comparatively larger amount of powders. In general, the mixing time should be amplified for getting the uniformity of cement paste in concrete.

For expressing the mixture of concrete, the authors adopted the normalized volume fraction of each component. As for gravel,  $C_g$  is defined as the volume fraction (concentration). Here, let us define the specific volume fraction  $C_g/C_{g,lim}$  normalized by the maximum gravel volume  $C_{g,lim}$  obtained by standardized dry rod compaction test<sup>10)</sup>. The specific volume fraction of gravel represents the compactness of gravel particles suspended in fresh concrete. This has been adopted as an indicator of the volume-based mix design of concrete mainly with respect to workability. Since

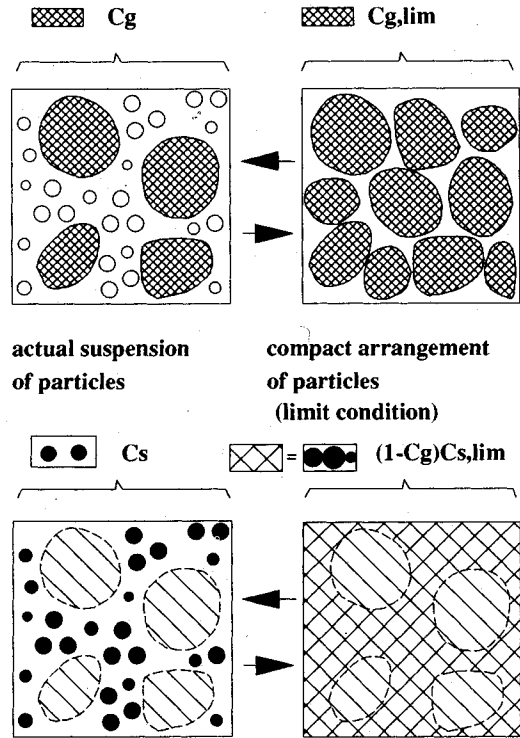


Fig.4 Indication of compactness of gravel and sand.

the dispersion of sand and powders is closely associated with the pumpability as well, indicators for dispersion of finer components will be meaningful.

Similarly, we can define sand volume fractions  $C_s$  and  $C_{s,lim}$  with the same manner. Here, the presence of gravel must be noted when computing the mechanical compactness of sand suspended by the finer particles (cement paste). Since sand component as the finer one can exist among voids of gravel, the allowable maximum volume fraction of sand is  $(1-C_g)C_{s,lim}$  under the presence of gravel in concrete. Accordingly, the specific volume fraction of sand denoted by  $C_s/(1-C_g)C_{s,lim}$  can represent how loosely the sand particles are suspended in the mortar matrix of concrete as shown in Fig.4. We can assume the infinite stiffness of fresh concrete concerning pumpability if either of the specific volume fraction of aggregates reaches unity.

With the same manner, the volume fractions of powder and the free water which is not restrained by the solids at inside are defined as  $C_b$  and  $C_w$ . In this study, the water to powder ratio denoted by  $C_w/C_b$  is used as an indicator of the mechanical property of paste among the voids of aggregates.

All mixtures are listed in Table 2 with the value of slump or slump flow and the pressure excited by

Table 1 Properties of Aggregates.

Specific gravity	Water Absorp(%)	Max. solid volume (%)	>5.0mm (%)	>2.5mm (%)	>1.2mm (%)	>0.6mm (%)	>0.3mm (%)	>0.15mm (%)	FM
2.53	1.7	69.0	1	12	32	62	89	98	2.94

Kind (gravel)	Specific gravity	Water Absorp(%)	Max. solid volume (%)	>20mm (%)	>15mm (%)	>10mm (%)	>5mm (%)	FM
crushed river	2.63	1.8	61.7	0	40	75	100	6.51
	2.62	1.19	64.3	0	40	75	100	6.51

Table 2 Test series.

Name	$\frac{C_g}{C_{g,lm}}$ (%)	$\frac{C_r}{(1-C_g)C_{r,lm}}$ (%)	$\frac{C_s}{C_s}$ (%)	powder	Adm. (%)	Slump (cm)	Flow (cm)	Air (%)	Temp. (°C)	Pressure (kgf/cm <sup>2</sup> )	Speed (cm/s)	Type of pipe
CMIX2	47c	69	110	C	2	27	76X75	1.3	21	0.495	5.56	T2.86
CMIX5	46c	68	126	C	1	25	47X44	0.7	20	0.434	5.56	T2.86
27MIX1	52c	70	110	F	-	23	55X53	0.5	21	0.072	6.30	T2.86
27MIX2	51c	68	109	S3	1	26	72X65	1.5	19	0.447	5.56	T2.86
27MIX4	51c	68	109	S8	1	24	50X50	1.8	19	0.458	5.00	T2.86
29MIX6	56r	70	89	CSF	.95	22	36X39	1.5	21	1.15	4.80	T2.86
29MIX8	49r	69	88	CSF	.95	26	59X62	2.1	20	0.547	5.26	T2.86
30MIX3	51r	73	109	CSF	1.1	24	42X43	2.2	20	0.743	5.26	T2.86
30MIX9	53c	78	95	CSF	.95	24	43X43	1.3	19	0.791	5.00	T2.86
30MIX7	54c	70	89	CSF	.95	25	57X57	1.5	19	0.768	5.00	T2.86
30MIX8	54c	63	84	CSF	.95	26	60X59	1.1	19	0.761	5.20	T2.86
BT1	50r	70	112	C	1.0	24	38X38	2.5	16	1.569	4.00	B
TP2	50r	70	112	C	1.0	25	53X54	2.5	16	1.300	4.00	T1.43
19TP	50r	70	142	C	1.0	-	60X60	1.8	14	0.122	5.25	T1.43
19BB	50r	70	142	C	1.0	-	60X60	1.8	14	0.157	5.00	B
22TP2	50r	70	122	C	1.0	-	54X54	3.1	13	0.279	5.00	T1.43
22BB2	50r	70	122	C	1.0	-	54X54	3.1	13	0.591	4.76	B
25TP	50r	70	100	C	1.0	4	-	1.5	14	1.017	3.85	T1.43
25BB	50r	70	100	C	1.0	4	-	1.5	14	1.175	4.00	B
26TP	60r	70	142	C	1.0	19	40X40	2.3	11	0.708	4.00	T1.43
26BB	60r	70	142	C	1.0	19	40X40	2.3	11	0.695	3.85	B
26TP2	60r	70	122	C	1.0	20	37X37	2.4	13	0.545	4.55	T1.43
26BB2	60r	70	122	C	1.0	20	37X37	2.4	13	0.790	4.35	B
BB1	40r	70	112	C	1.0	-	59X59	1.9	27	0.532	5.56	B
BB2	50r	70	112	C	1.0	22	40X40	1.5	28	0.594	5.26	B
TPB2	50r	70	112	C	1.0	22	40X40	1.5	28	0.722	5.00	T2.86
BB3	60r	70	112	C	1.0	18	30X30	1.0	28	0.732	5.00	B
BB5	65r	70	112	C	1.0	3	-	1.0	29	0.854	3.85	B
BB6	60r	60	112	C	1.0	-	62X62	1.0	28	0.519	5.56	B
BB9	60r	70	112	C	1.0	18	29X29	1.3	26	0.655	5.00	B
TBB9	60r	70	112	C	1.0	18	29X29	1.3	26	0.773	5.00	T1.43
BB10	65r	70	112	C	1.0	5	-	2.7	27	1.340	2.00	B
TBB10	65r	70	112	C	1.0	5	-	2.7	27	0.951	4.35	T1.43
TBB11	60r	65	112	C	1.0	-	22X22	1.0	23	0.636	5.00	T1.43
BB11	60r	65	112	C	1.0	-	22X22	1.0	23	1.022	5.00	B
TP	60c	70	112	C	1.0	13	-	2.5	22	0.717	5.00	T1.43
TP3	60c	70	112	C	1.0	13	-	2.5	22	1.665	4.55	T2.86
TP4	60c	75	112	C	1.0	16	-	2.2	21	0.970	5.00	T1.43
TP5	60c	75	112	C	1.0	16	-	2.2	21	2.000	4.00	T2.86
TPF1	60c	60	112	C	1.0	21	-	1.2	21	1.049	5.00	T2.86
TPF3	60c	60	112	C	1.0	21	-	1.2	21	0.922	4.00	T2.86
TFS1	50c	70	112	C	1.0	-	64X64	2.9	23	0.390	5.56	T1.43
TPL1	50c	70	112	C	1.0	-	64X64	2.9	23	0.768	5.00	T2.86
TFS2	50c	80	112	C	1.0	11	22X22	2.0	23	0.778	5.38	T1.43
TPL2	50c	80	112	C	1.0	11	22X22	2.0	23	1.790	5.38	T2.86
TFS8	63c	70	112	C	1.0	19	29X29	1.9	20	0.982	5.00	T1.43
TPL8	63c	70	112	C	1.0	19	29X29	1.9	20	2.450	4.59	T2.86

1) gravel : c - crushed, r - river

2) powder : C - cement, F - fly ash, S3 - slag 3000, S8 - slag 8000, CSF - cement 30% + slag3000 30% + fly ash 40% by weight

3) BT1 & TP2 : tested 1 hour after mixing, and others 10 minutes after mixing

4) Pozzolith SP-9HS was used.

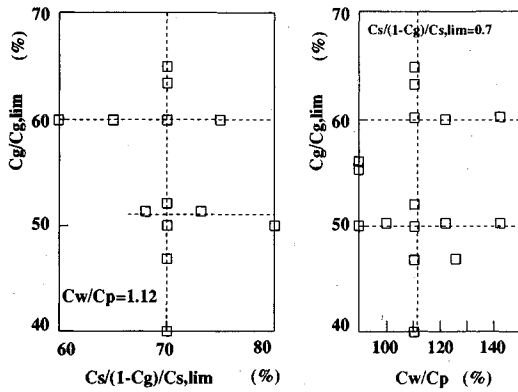


Fig.5 Range of mixture proportion.

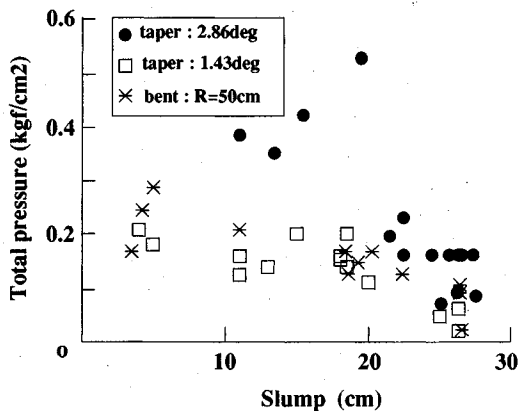


Fig.6 Relation of total pressure and slump.

the pure shear deformation of concrete around tapered or bent pipe units. The most rate of flow ranged from 4.5 to 5.5cm/s. The pressure listed is the oil pressure after deducting the resistance component arising at the straight pipe as ( $P_c - P_w$ ). Then, the total pressure applied to concrete is 0.215 times the oil pressure listed.

Fig.5 shows the extent of the specific volume fractions of gravel and sand adopted and the water to cement ratio by volume. Since the mixtures cover conventional as well as the highly fluidized concrete, the slump varies from 3cm to approximately 27cm with 64cm slump flow. These values were obtained just before starting the pumping test. Some of tests were carried out one hour after charging concrete inside the pump cylinder. Then, the slump, slump flow and the measured response differ despite of the same mix proportion and the procedure of production.

The relations of the total pressure and the slump are shown in Fig.6 according to the boundary conditions. The general trend, i.e., the greater slump gives rise to the lower pressure, is seen, but much deviation of data exists. Roughly speaking,

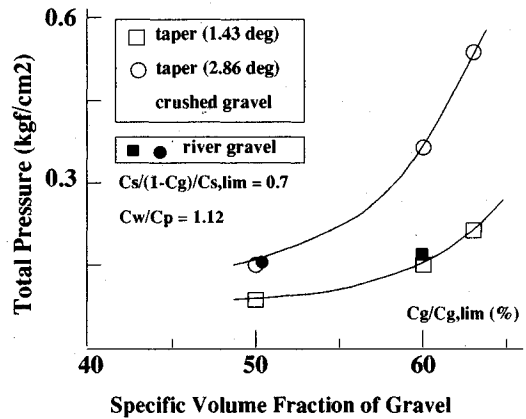


Fig.7 Effect of volume content of gravel on the total pressure at tapered pipes.

the taper unit with 1.43° of the tapering angle looks similar to the case of bent pipe with the radius 50cm. The boundary condition corresponding to 2.86° of the tapering angle resulted in the highest resistance among the tested conditions adopted. The pressure loss made by the deformed pipe units corresponds to the pressure loss caused by the straight pipe of several meters long.

But, more or less, the total pressure to indicate the deformational resistance is not unique no matter what the value of slump is produced. This means that the slump of concrete under gravity cannot always be the indicator of pumpability. In fact, the value of slump serves as crude indicator for pumpability, but insufficient for being devoted to the engineering practice. It is indispensable to explore the relation between the pressure necessary for stable flow and the concrete mixtures with the aid of dynamics of particulate flow. For this purpose, the multi-phase concept<sup>5)</sup> will be crucial for naturally incorporating the mixture proportion of fresh concrete.

### 3. VOLUME FRACTION OF GRAVEL AND DEFORMABILITY

For discussing the effect of compactness of gravel, the authors picked up the pressure data of ordinary Portland cement concrete as shown in Fig.7 (tapered pipe). As the specific volume fractions of sand and water to powder ratio were common, i.e., mortar mix proportion remained constant in concrete with different specific volume fractions of gravel, the stress transfer concerning the collision and friction of gravels will be changed. The higher concentration of gravel gives exponential rise to the resistance against the deformation realized in tapered pipes under constant rate of flow.

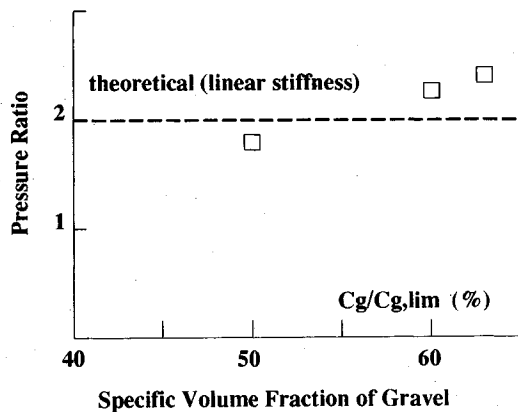


Fig. 8 The ratio of total pressure made at tapered pipes with different tapering angles.

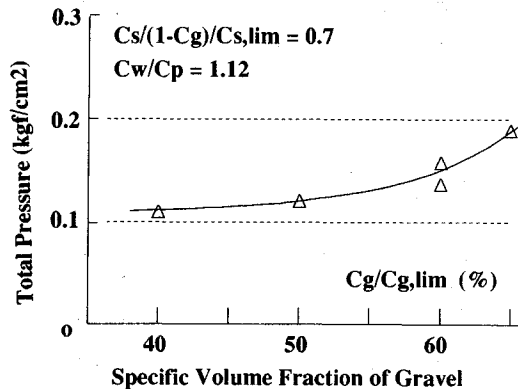


Fig. 9 Effect of volume fraction of gravel on the total pressure at bent pipe.

In Fig. 7, the same resisting pressure was observed for river and crushed gravels when we use the specific volume fraction of aggregates, which are thought to indicate the compactness of particulate suspension based upon multi-phase concept. This result was also reported in terms of the shear stiffness of the single phase sands obtained from several places<sup>10</sup>. Strictly speaking, the correlation of the specific volume fraction and the stiffness or pumpability may differ unless the shape, surface roughness and others would be the same. But, as an extreme case, the unity of specific volume fraction always provides the infinite stiffness and no deformability indeed.

For the time being, we can use the normalized volume content of aggregates as indicators related to the stiffness and the deformability. It can be generally said that the maximum solid volume fraction implicitly represents the grading and shape of particles. Within this study, it does function well as normalization factor for representing the interaction of particles.

It is clear in Fig. 7 that the steeper angle of taper produces the higher pressure. From the visualized test of dense solid liquid mixture, the shear mode deformation of particle assembly was manifested and its magnitude was quantified in 2-dimensional space<sup>9</sup>. Based on this investigation and axisymmetry of flow field, 3-dimensional shear intensity was proposed as<sup>9</sup>,

$$J_{\theta} = \frac{\sqrt{3}}{r} \tan \theta \cdot u \dots \dots \dots (1)$$

where,  $J_{\theta}$  and  $u$  represent the sectional averaged shear rate and flow rate of the liquid-solid flow. The values of “ $r$ ” and  $\theta$  are the pipe radius of the section concerned and the taper angle, respectively.

Theoretically speaking, the rate of flow denoted

by “ $u$ ” is different in each section although the mean rate of flow at the inlet remains constant. The value of “ $r$ ” is also variable. Due to smaller tapering angle, however, those values can be nearly the same. Then, the steeper tapered pipe (2.86 degree) may generate the greater shear intensity than that of 1.43 degree and its ratio is close to,

$$\frac{J_{\theta}(\theta=2.86^{\circ})}{J_{\theta}(\theta=1.43^{\circ})} \cong \frac{\tan 2.86^{\circ}}{\tan 1.43^{\circ}} = 2 \dots \dots \dots (2)$$

The pressure increasing ratio of tapered pipes are shown in Fig. 8 including six different mixtures. Actually, the ratio of the pressure between two taper angles is close to the above mentioned ratio in terms of shear intensity. It may be reasonable to conclude that the resistance to the deformation specified by the pressure is nearly proportional to the shear rate intensity obtained in the pipe units when we have lower rate of flow compared with that realized in practice.

Fig. 9 shows the sensitivity of the specific volume fraction of gravel to the pressure caused by the bent pipe. It seems that the gradual increase in the total pressure is obtained according to the increasing volume fraction of gravel. Roughly speaking, the pressure induced by the bent pipe (bent radius = 50cm) is similar to those generated by the tapered pipe unit with 1.43 degree of tapering angle.

#### 4. VOLUME FRACTION OF SAND AND DEFORMABILITY

The relation of the pressure versus the specific volume fraction of sand is shown in Fig. 10, Fig. 11 and Fig. 12, in which the specific volume fraction of gravel and water to cement ratio by volume were intentionally made constant.

Even though the sand content is changed, the pressure obtained by greater tapering angle (2.86 degree) is about two times that by small angle (1.43

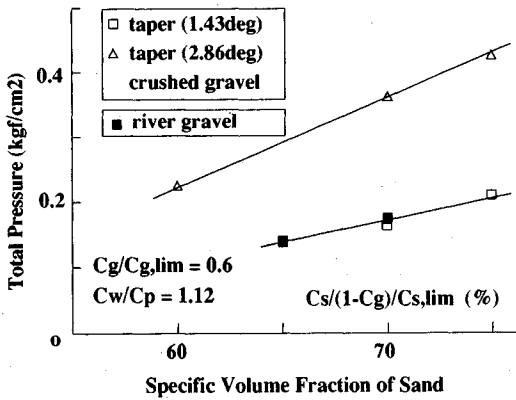


Fig.10 Effect of volume fraction of sand on the total pressure at tapered pipes.

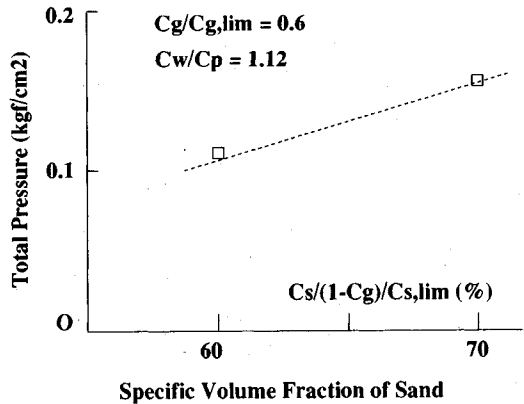


Fig.12 Effect of volume content of sand on the total pressure at bent pipe.

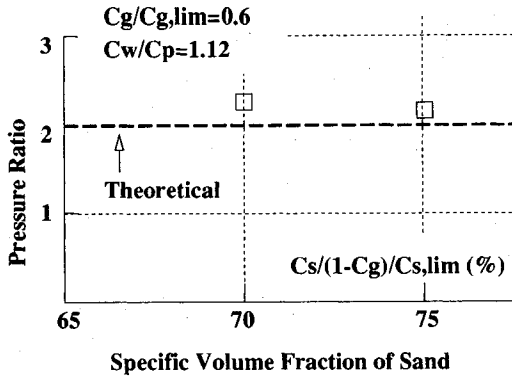


Fig.11 The ratio of total pressure made at tapered pipes with respect to the volume content of sand.

degree) similar to the case in Chapter 3. The specific volume fraction of sand adopted is also proved to be effective for covering different types of aggregates as shown in Fig.10. In Fig.11, since the gravel suspension is common, we can assume that the coarser component may have the same contribution to the total stiffness. This means that the different total pressure made by different taper angles originates from the load carrying mechanics of finer component. Accordingly, we can guess that the sand stiffness is also directly associated with the rate of shear of coarser component.

In comparison with the specific volume fraction of gravel, it is noted that the higher compactness of sand is possible to maintain the pumpability to some extent. When we specify the volume fraction of gravel greater than 65% of the limit, sudden drop of pumpability was underwent and accompanied by the elevated pressure over the capacity of the machine as long as the authors run the series of experiment.

On the other hand, the greater volume inclusion

of sand than 75% of the limit does not matter. If the lower volume fraction of sand would be specified, we may encounter the settlement of coarser particles under static condition. As far as the particles interaction is concerned, there exists some size effect on the deformability of concrete.

It would be acceptable that the relative size of the particles compared with the referential dimension has much to do with the stress transfer through particles. In fact, the gravel is supposed to bear stress which is transferred through contact and friction, and is supported by the wall of pipes. The ratio of the particles to the dimension of pipes may influence on this contact mechanism, quantitatively. In general, the size ratio of sand to the typical dimension of flow is quite smaller than that of gravel. The assumption that the gravel assembly can admit no easier deformation than sand will make sense. For the time being, the pressure measured is to be understood as particular one associated with the size of pipe diameter and the maximum size of aggregates.

As other factor, the coarser particles will generate the larger scale eddy and turbulence which is associated with the additional momentum transfer across the section. The induced momentum transferred by the inertia of particulate turbulence through the flow section generates the additional stress. This term is reflected by the increased value of stiffness in appearance and implicitly considered in the constitutive model<sup>15</sup>.

### 5. KINDS OF POWDERS AND DEFORMABILITY

The mechanical properties of paste in concrete are determined by the kind of fine powder, volume fraction of powder in paste, dosage of chemical admixture agents and the procedure of production



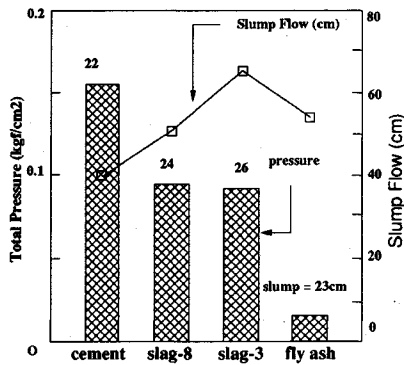


Fig.13 Kinds of powders on the total pressure at the tapered pipe (2.86 degree) :  $C_g/C_{p,lim}=0.5$ ,  $C_s/(1-C_g)/C_{s,lim}=0.7$  and  $C_w/C_p=1.12$ .

such as mixing efficiency. The authors adopted four different kinds of powder particles, e.g., ordinary Portland cement (Blaine=3000), blast furnace slag (Blaine=3000, and 8000) and fly ash. Fig.13 shows the effect of powders on the deformability denoted by the pressure. Since the volume fractions of aggregates and water to powder ratio by volume were intentionally maintained equal, the different pressure was caused by the paste mechanics in concrete.

What we should pay attention to is the correlation of the pressure and the slump with regard to the powder in kind. As shown in Fig.13, the values of slump of slag (Blaine 8000) and fly ash concrete are close to each other. In spite of the fact that the similar deformability was attained under the gravity action, the pressure, which is obtained under comparatively higher interaction of particles, was dropped so much when fly ash was used.

Let us compare the case of slag with Blaine 3000 with fly ash concrete. As long as the slump carried out under gravity, the consistency of slag concrete (3000) is better than that of fly ash concrete. However, the slag concrete exhibits approximately four times greater pressure when the concrete passed through the tapered pipes than the one of fly ash concrete.

The above mentioned inconsistency between slump and the measured pressure will be owing to the different level of shear rate and the inter-particle force. It can be guessed that the shape of the powder is much sensitive to the deformation accompanying greater shear frictional contact among aggregates as well as between aggregates and pipe walls<sup>12)</sup>. Here, the volume fraction of aggregates associated with the mean distance of suspended particles may affect on this powder sensitivity too.

The mixed cementitious powder consisting of

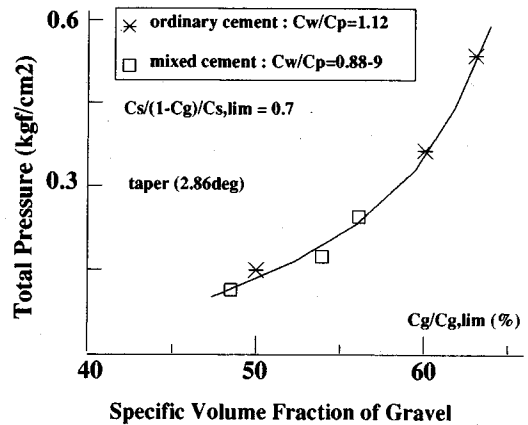


Fig.14 Kinds of powder on the total pressure and aggregate content.

ordinary cement, fry ash and blast furnace slag (specified as CSF in Table 2) were reported to be a key to bring higher workability<sup>2)</sup> too. In other words, the replacement of ordinary cement with the blended one reduces the water content enough to yield some similar deformability as shown in Fig.14. Approximately 90% of the water to mixed powder ratio by volume is equivalent to 112% of that for pure ordinary Portland cement concrete. It was examined that pure ordinary cement concrete having 90% of the water to cement ratio loses deformability for passing through the tapered pipe within the pumping capacity of the apparatus as shown in Fig.2. It was reported through reference<sup>2)</sup> that the concrete mixtures with mixed type powder used in Fig.14 satisfy the self-placable requirement which is essential among several requirements of High Performance Concrete.

It has to be said that the relation as shown in Fig.13 and Fig.14 depends on the grading and shape of powders. In future, the indicator to represent the physical characteristics of powder is strongly required. The concept of effective free water by Ozawa et al.<sup>2)</sup> is one of proposals.

## 6. VOLUME FRACTION OF POWDER AND DEFORMABILITY

From the above mentioned results, it can be concluded again that the consistency and the pumpability are not directly associated<sup>13)</sup>. For deriving the mechanical role of paste in pumpability from the experiments, the authors focused on the sensitivity of the volume fraction of powder to the concrete pressure needed to maintain the same mode and magnitude of deformation as shown in Fig.15 and Fig.16. For both bent and tapered units, the greater water to cement ratio by volume reduces the pressure provided the smaller volume

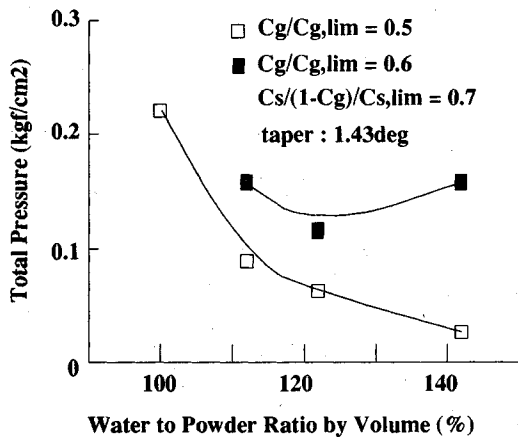


Fig.15 Effect of water to cement ratio on the total pressure at the tapered pipes.

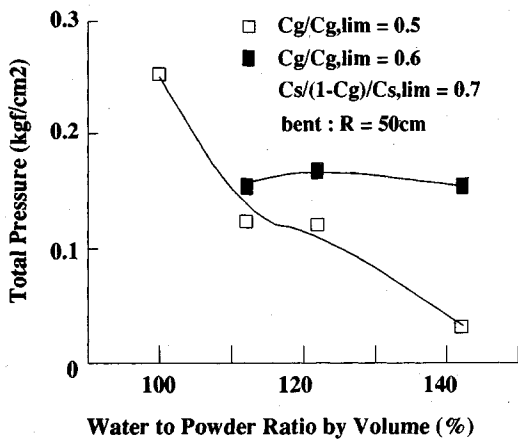


Fig.16 Effect of water to cement ratio on the total pressure at the bent pipe.

fraction of gravel ( $C_g/C_{g,lim}=0.5$ ). It can be guessed that the reduction of the stiffness of cement paste is the source of the lower resistant concrete, because the paste is one resisting component of fresh concrete against shear.

As for the case of 60% of the specific volume fraction of gravel, the greater total pressure was generated due to the closer distance between gravels. However, the tendency in terms of paste property is very different indeed from the lower compactness of gravel as shown in Fig.15 and Fig.16. Despite of the higher consistency of paste produced by greater water to cement ratio, the concrete pressure as a whole was elevated rather than decreased when the larger amount of coarse aggregate is specified. If we would accept the resistant mechanism of paste matrix without any interaction with suspended aggregate components, this apparent behavior cannot be consistently

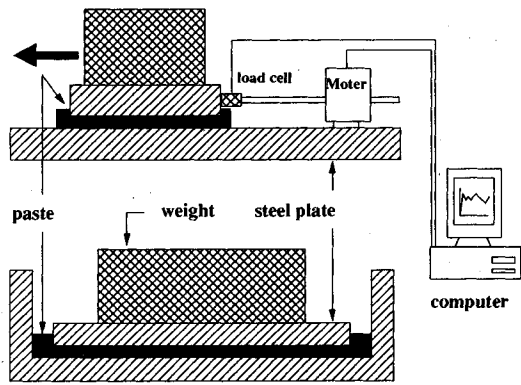


Fig.17 Set-up of paste friction test.

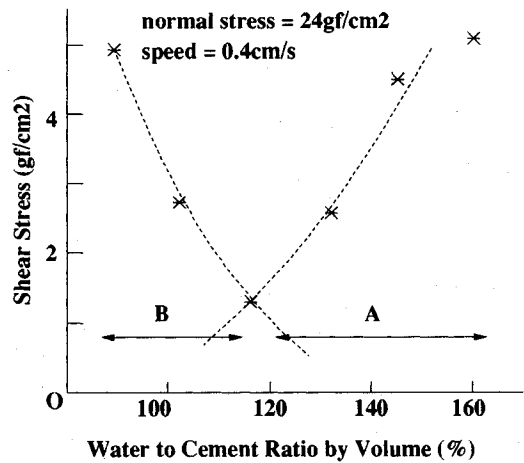


Fig.18 Transferred shear stress through the paste.

explained.

Concrete with the higher volume fraction of gravel will comparatively bear greater interacting forces through the gravel phase. Then, the stress transferred by the contact of gravel will be the main part of the resistant mechanism compared with the consistency of paste<sup>19</sup>. One of the possibility to explain the above nonlinearity is the role of paste on the stress transfer through the particles of gravel. Cement paste is present around the contact point of gravels and may serve as the lubrication agent as well as the matrix with its own consistency achieved by the powder to powder contact. If the amount of gravel is less, the latter role of paste will be prominent, and vice versa.

For verifying the hypothesis above, the authors conducted the direct shear test of paste<sup>10</sup> with the device as shown in Fig.17. This test was designed so as to reproduce the frictional contact of solids with the paste. The upper steel plate which held cement paste with the bottom plate was driven by the servo motor through a rod as shown in Fig.17.

The horizontal force was measured in time domain. Through the time averaging process during 5 seconds, the mean force was decided. The frictional shear stress, which is the time averaged shear force normalized by the area of shear plane, was obtained under the constant normal compression maintained by the weight of mass.

The relation of the transferred shear stress through the paste and the water to cement ratio is shown in Fig.18. The minimum friction is seen at particular water to cement ratio. Although the less volume fraction of cement gives rise to the low stiffness of the paste itself and reduced stress transfer at zone B as shown in Fig.18, it brings higher friction at zone A. At zone A, the frictional shear may be transferred chiefly through the direct contact between solid plates. Otherwise, some of powder particles may lie between contact points of plates. It can be concluded that the cement paste acts as the phase with its characteristic resistance to deformation corresponding to zone B as well as the agent to characterize the stress transfer of coarser components like a coating material.

## 7. CONCLUSIONS

The deformation induced by the flow of fresh concrete was reproduced in the tapered and bent pipe units with different dimension and the pressure needed was measured for approximately 20 different mixtures. The following conclusions were drawn by collecting fundamental data to form the stiffness model for flow analysis of fresh concrete.

(1) The specific volume fraction of aggregates were proved to be an appropriate parameter for generalizing the pumpability and the resistance to deformation. Since the river and crushed gravel have different shapes and grading, the pressure generated by the deformed pipe units is different even if the mixture by volume is equal. However, the same specific volume fraction, which is the normalized one by the maximum volume fraction corresponding to the dry rod compactness, was verified to indicate the same deformability specified by the pressure.

(2) The pressure needed through tapered pipes was found to be directly proportional to the sectional averaged shear rate which is the function of the taper angle and the rate of flow. In considering that the resistance to deformation is mainly caused by the particle collision and friction, it is guessed that the interaction force of particles in fresh concrete is nearly linear to the shear rate in the tapered pipe units.

(3) In spite of the fact that the pressure

monotonically varies according to the specific volume fraction of gravel and sand, there exists some particular water to cement ratio which gives rise to the minimum resistance to deformation provided the higher volume content of gravel. But, the optimum water to cement ratio does not appear if the lower compactness of gravel, e.g., the lower particle interaction, is specified. Accordingly, it can be concluded that the paste in fresh concrete not only produces the resistance as the matrix suspending aggregates similar to the gravels, but also affect on the frictional contact of coarser particles. This interaction among constituent phases of fresh concrete was indirectly verified by the direct shear test of cement paste under steady rate of shear.

(4) The pressure excited by the deformation of concrete was influenced so much by the sort of powder. Fly ash was found to reduce the pressure which gets about 20% of the pressure for blast furnace slag. The frictional contact force of aggregates may be degraded because of the round shape of fly ash. However, the consistency expressed by slump were not different very much, approximately 80 - 110% of the slump value of slag concrete.

No correlation between the pumping resistance and the slump was manifested. The above mentioned inconsistency will be owing to the different level of shear rate and the inter-particle force. It can be guessed that the shape of the powder is much sensitive to the deformation accompanying greater shear frictional contact among aggregates as well as between aggregates and pipe walls.

## ACKNOWLEDGMENTS

The authors express their sincere gratitude to Prof. H. Okamura, The University of Tokyo, for his valuable suggestions. This study was fully supported by the Grant-in-Aid for Scientific Research No.8795443 from the Ministry of Education, and the financial aid on it was also granted to the last author by Japan International Cooperation Agency during his secondment to Asian Institute of Technology.

## REFERENCES

- 1) Okamura, H. : Waiting for innovation in concrete materials, *Cement and Concrete*, No.475, pp.2-5, Sept., 1986 (in Japanese).
- 2) Ozawa, K., Maekawa, K. and Okamura, H. : Development of high performance concrete, *Journal of the Faculty of Engineering, The University of Tokyo (B)*, Vol.XLI, No.3, 1992.
- 3) Hashimoto, C., Maruyama, K. and Shimizu, K. : Study on

- visualization of blockage of fresh concrete flow in pipe, Concrete Journal, Vol.26, No.2, 1988. (in Japanese)
- 4) Ozawa, K., Nanayakkara, A. and Maekawa, K. : Evaluation of aggregate particle motion in liquid-solid flows of model concrete, Proc. of JSCE, No.408/V-11, pp.187~193, Aug., 1989.
  - 5) Nanayakkara, A., Ozawa, K. and Maekawa, K. : Deformational compatibility of aggregate phase for tapering flow of dense liquid-solid material, Proc. of JSCE, No.420/V-13, pp.279~290, Aug., 1990.
  - 6) Nanayakkara, A., Ozawa, K. and Maekawa, K. : Deformational compatibility for solid phase of dense liquid-solid flow in bend pipes, Proc. of JSCE, No.426/V-14, pp.221~232, Feb., 1991.
  - 7) Maekawa, K., Ozawa, K. and Nanayakkara, A. : Solid stiffness model for analysis of fresh concrete flow : gravel, sand and cement slurry mixture, 4th Int. Symposium on Liquid-Solid Flows, ASME, FED-Vol.118, pp.39~44, 1991.
  - 8) Nanayakkara, A., Ozawa, K. and Maekawa, K. : Flow and segregation of fresh concrete in tapered pipe : Two phase computational model, 3rd. Int. Symposium on Liquid-Solid Flows, ASME, FED-Vol.75, pp.47~52, 1988.
  - 9) Isshiki, M., Yamazaki, M. and Okamura, H. : The deformation of fresh concrete pumped through pipe lines, Concrete Library of JSCE, JSCE, No.7, pp.65~78, July, 1986.
  - 10) For example, Japan Industrial Standard (JIS) A1104, or JSCE specification -Standards-, JSCE, 1991.
  - 11) Seed, H. B. and Lee, K. L. : Liquefaction of saturated sands during cyclic loading, Proc. of ASCE, Vol.92, SM6, pp.105~134, 1966.
  - 12) Tanabe, K. and Takase, S. : Bifurcating pipe layout method for concrete pumping, Concrete Journal, Vol.25, No.6, June, 1987 (in Japanese).
  - 13) Working group on recommendation for pumping methods in the sub-committee on construction practice of JSCE, Recommended practice for pumping concrete, Concrete Library of JSCE, No.8, pp.1~34, December, 1986.
  - 14) Ma, D. N. and Roco, M. C. : Probabilistic three-dimensional model for slow shearing particulate flow ; wet friction, 3rd. Int. Symposium on Liquid-Solid Flows, ASME, FED-Vol.75, pp.53~58, June, 1988.
  - 15) Nanayakkara, A. S. N. : Computational model for pumpability of concrete, Doctoral Dissertation submitted to The University of Tokyo, 1990.
  - 16) Izumi, T., Maekawa, K., Ozawa, K. and Kunishima, M. : Influence of paste on the frictional resistance between solids, Proc. of JCI, Vol.10, No.2, pp.309~314, 1988. (in Japanese)

(Received March 26, 1992)

## ベント管およびテーパ管を流れるフレッシュコンクリートの 変形抵抗

ナナヤッカラ アヌラ・小沢一雅・前川宏一

本文はフレッシュコンクリートのせん断場における変形抵抗性を、多相・多要素流動体の概念から整理することを目的とする。ベントおよびテーパ管内にコンクリートを強制流動させることで純せん断場を再現するとともに、対応する変形抵抗性を圧力降下の形で定量化した。骨材・粉体・液相の体積比と、その種類を広範に変化させたコンクリートの変形性が報告されている。ここで、変形管内での変形適合条件とコンクリート中の固体粒子群のせん断抵抗則から、変形抵抗性を表現できることが示唆された。